Suppressing RF Front-End Nonlinearities in Wideband Spectrum Sensing

Eric Rebeiz[†], Ali Shahed hagh ghadam[*], Mikko Valkama[*], and Danijela Cabric[†]
[†] University of California Los Angeles, CA, USA
[*] Tampere University of Technology, Finland
Email: {rebeiz, danijela}@ee.ucla.edu, {ali.shahed, mikko.e.valkama}@tut.fi

Abstract— As a result of wideband analog front-end, wideband spectrum sensing techniques are prone to suffer from RF non-linearities. Intermodulation products due to strong subbands or carriers stemming from low noise amplifier nonlinearities, can easily degrade the spectrum sensing performance by causing false alarms and degrading the detection probability. We analyze the effects of third-order nonlinearities on both energy detectors and cyclostationary detectors under front-end nonlinearities. We show that the presence of strong blockers in the wideband channel can substantially degrade the sensing performance of both detectors, and energy detectors loose their advantage over cyclostationary detectors. Then, we propose an adaptive interference cancellation algorithm to compensate for the effect of the blockers at any subband of interest. The obtained results also show that when compensation is enabled, cyclostationary detector is more robust to moderate blocker signal levels than the corresponding energy detector.

I. INTRODUCTION

In the context of Cognitive Radios (CRs) [1], secondary users (SUs) sense the spectrum to opportunistically access the unused subbands. However, SU must avoid interfering with the licensed Primary Users (PUs). As a result, spectrum sensing [2] is key to the deployment of future cognitive radios. The RF front-end of the sensing radios can either support narrowband or wideband sensing. Narrowband RF front-ends allow the sensing radios to tune to a single subband at a time. In such an approach, sensing would require tuning of the local oscillator used for downconversion, and only a single channel can be sensed at a time. On the other hand, wideband RF font-ends downconvert a wide range of frequencies to baseband, where the filtering is performed digitally. In such receivers, sensing multiple subbands would entail changing the filtering performed in DSP only while keeping the RF front-end untouched. In particular, we focus in this work on wideband RF front-ends as sensing multiple subbands can be performed purely on the digital side.

With respect to different techniques for spectrum sensing [2], cyclostationary-based detectors (CD) [3], [4] rely on detection of hidden redundancies in the received signal. The redundancy is captured by correlating the received signal with a frequency-shifted version of itself. The frequency by which the signal is to be shifted before correlating it with itself, referred to as cyclic frequency, is a function of the signal's modulation type, its symbol rate, and carrier frequency, all of which are assumed to be known. On the other hand, energy detectors (ED) [5] rely on computing the energy in the subband of interest to determine whether the signal of interest (SOI) is present or not by comparing it to a threshold. Although energy detectors require the least amount of information about the signal to be detected, they do suffer from the noise uncertainty problem [6] when the noise floor cannot be estimated accurately. Cyclostationary detectors do not suffer from the noise uncertainty problem, and are therefore more robust than energy detectors in this regard.

The effects of certain receiver front-end non-idealities such as phase noise [7] and I/Q imbalance [8] as well as sampling clock offset on the performance of signal detectors have been reported in number of studies, e.g. [9], [10]. The assumption in these studies is that the receiver operates in its linear region. However, depending on the received power of the incoming signal, wideband sensing receivers might operate in a range where the RF front-end components such as Low Noise Amplifier (LNA) exhibit a non-linear behavior. Therefore, spurious frequencies in the form of harmonics, intermodulation (IM) and crossmodulation (XM) are generated [11], [12]. As a result, the presence of strong blockers, i.e. strong signals inside or outside the subband of interest, in the wideband spectrum produces distortion terms that affect the detection performance in other subbands where weaker signals may reside [12], [13]. Under such scenarios, the detection performance might be degraded, causing the CR network to either cause harmful interference to the PU, or to miss the opportunity to transmit in a vacant subband. In [14], [15] an Adaptive Interference Cancellation (AIC)-based algorithm is used to compensate for the front-end nonlinearities. However, these papers, generally, demonstrate the performance of AIC only in terms of IMD mitigation and, to the authors knowledge, there are no studies available on the performance of the spectrum sensing algorithms with/without the AIC algorithm, which is the focus of this paper.

The aim of this paper is to study the robustness of different spectrum sensing techniques to non-linear RF front-ends. We show that strong blockers can severely degrade the sensing performance for both cyclostationary-based detectors and energy-based detectors. We describe in Section II the system model and formulate the detection problem to be solved. Section III presents both kinds of detectors to be studied in this work, and shows the degradation in sensing performance under third-order nonlinearities. Section IV describes the adaptive technique for interference cancellation to reduce the effect of

the blockers in the subband of interest. We show in Section V the performance gains when using the proposed solution, and Section VI concludes the paper.

II. SYSTEM MODEL

The problem of receiver (Rx) front-end nonlinearity in the sensing of a wideband spectrum on channel-by-channel basis is considered in this article. In this scheme, the entire wideband signal is downconverted to baseband and digitized. Then, digital filtering is performed for the subband of interest, and the resulting I/Q samples are fed to the detector to perform spectrum sensing. Naturally, the nonlinearity in the sensing front-end results in the generation of intermodulation (IM) terms. As a result, the IM terms can affect the performance of the sensing Rx in terms of degradation in receiver operating characteristic (ROC) curve for a given signal-to-noise ratio (SNR). The odd-order nonlinear terms are only considered for the modeling of the RF front-end nonlinearity as the spurious frequency components that are generated by the even-order terms, i.e harmonics and inter/cross-modulation terms, are assumed to be outside of the overall digitized wideband [11]. Moreover, the nonlinearity in the front-end is assumed to be mild and therefore is modeled with a cubic term. As a result, the baseband equivalent of the wideband signal at the output of the nonlinear front-end can be described as [15]

$$y_W[n] = \beta_1 x[n] + \beta_3 x[n]|x[n]|^2 + w[n], \quad (1)$$

where β_1, β_3 are characteristics of the sensing Rx front-end, $x[n]$ is the received baseband equivalent wideband signal, and $w[n]$ is the additive white Gaussian noise. The values for β_1, β_3 are related to the amplitude A_{IP3} of the signal at third-order intercept point through the following expression [15]

$$A_{IP3} = \sqrt{\frac{4|\beta_1|}{3|\beta_3|}}. \quad (2)$$

Also the power of the input signal $y_W[n]$, in dBm, and in terms of A_{IP3} can be written as [15]

$$P_{IP3} = 20\log_{10} A_{IP3} + 10 \text{ dBm}.$$

We focus on the detection of a given subband in the wideband spectrum centered at f_c. The licensed primary user that may occupy this channel utilizes a known modulation scheme. The real world example of such setup is the digital TV band in US where the primary users are single carrier signals with vestigial single sideband (VSB) modulation. As a result of the third-order nonlinearity, the third-order intermodulation term of any two relatively strong signals $z_i(t)$ and $z_j(t)$, also known as *blockers* in this context, located at f_i and f_j will fall in the subband of interest if $f_i \pm 2f_j = f_c$ or $2f_i \pm f_j = f_c$. We focus on the baseband representation of such a scenario in a given subband of interest after downconversion to an intermediate frequency f_{IF} and digital filtering. For example, in the single pair of blockers case, it was shown in [15] that the signal in the subband of interest is given by

$$y[n] \approx \left(\beta_1 z_0[n] + \frac{3\beta_3}{2} z_i^2[n] z_j^*[n] \right) e^{j2\pi f_{IF}nT_s} + w_z[n], \quad (3)$$
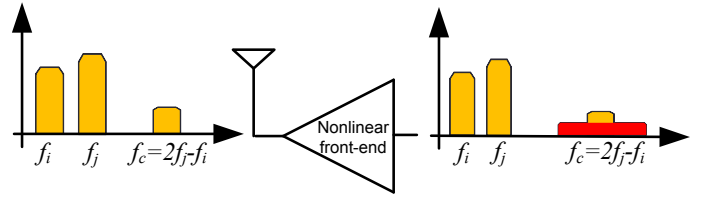

Fig. 1. Interference on the SOI by the IMD components that are generated by two blockers as the result of third-order nonlinearity in the receiver front-end. In this example blockers are around frequencies f_i and f_j. The SOI is around frequency $f_c = 2f_j - f_i$.

where $z_0[n]$ is the baseband version of signal of interest (SOI), $z_i[n]$ and $z_j[n]$ are the baseband representation of the blockers whose third-order IMD term falls in the subband of interest at center frequency $f_c = 2f_i - f_j$. The center frequency of the subband of interest after RF I/Q downconversion is denoted by f_{IF} and T_s is the sampling period. Finally, $w_z[n]$ is the complex white Gaussian additive noise in the subband of interest. It should be noted that in this model the assumption is that the blockers are orders of magnitude stronger than SOI, i.e. $\mathbb{E}[|z_0[n]|^2] \ll \mathbb{E}[|z_i[n]|^2]$. Therefore, the additional IMD terms around f_c generated by the SOI and one blocker in the form of $z_0[n]|z_i[n]|^2$ as well as the self-interference IMD term generated by the SOI in the form of $z_0[n]|z_0[n]|^2$ are negligible compared to the IMD terms of the blocker pairs. One example of the power spectrum density (PSD) of a two blocker case for a Rx front-end with finite IP3 is depicted in Fig. 1.

The goal of the CR is to detect the presence of the weak SOI $z_0[n]$ in the presence of strong blockers. The filtered signal under both hypotheses is given as follows

$$y[n] = \begin{cases} \frac{3\beta_3}{2} z_i^2[n] z_j^*[n] e^{j2\pi f_{IF}nT_s} + w_z[n], & \text{under } \mathcal{H}_0 \\ \\ \left(\beta_1 z_0[n] + \frac{3\beta_3}{2} z_i^2[n] z_j^*[n] \right) e^{j2\pi f_{IF}nT_s} \\ + w_z[n], & \text{under } \mathcal{H}_1. \end{cases}$$

We define the Signal to Noise Ratio (SNR) with respect to the SOI as

$$\text{SNR} = 10\log_{10} \left(\frac{\mathbb{E}[\beta_1^2|z_0[n]|^2]}{\mathbb{E}[|w_z[n]|^2]} \right) \text{dB}, \quad (4)$$

where $\mathbb{E}[\cdot]$ is the statistical expectation operation. Further, we assume for simplicity that both blockers have the same power, i.e. $\mathbb{E}[|z_i[n]|^2] = \mathbb{E}[|z_j[n]|^2]$, and define the Signal to Interference Ratio (SIR) as

$$\text{SIR} = 10\log_{10} \left(\frac{\mathbb{E}[|z_0[n]|^2]}{\mathbb{E}[|z_i[n]|^2]} \right) \text{dB}. \quad (5)$$

III. DETECTION METHODS AND PROBLEM FORMULATION

We consider energy detectors and cyclostationary detectors as the two detection methods to be analyzed. After defining the two detectors, we show the impact of RF nonlinearities on both detectors.

A. Spectrum Sensing Algorithms

Cyclostationary detectors (CD) rely on detecting the presence or absence of cyclic features in the received signal. In order to detect the presence of a cyclic feature, a typical detection method relies on the computation of the Cyclic Auto-Correlation (CAC) function. This detection method correlates the received signal with a frequency shifted version of itself at a given lag ν, where the cyclic frequency is denoted by α. For the case of linearly-modulated signals, the cyclic frequencies at which cyclic features occur are a function of the signal's symbol rate and carrier frequency. With a finite sensing time, the non-conjugate CAC $R^\alpha(\nu)$ is computed with N samples as follows

$$R_y^\alpha(\nu) = \frac{1}{N} \sum_{n=0}^{N-1} y[n]y[n-\nu]e^{-j2\pi\alpha nT_s}. \qquad (6)$$

For the signal class considered in this work, it was shown in [3] that VSB signals exhibit a cyclic frequency at $\alpha = 2f_{IF}$. Although the imperfect knowledge of the cyclic frequency degrades the detection performance of cyclostationary detectors as shown in [16], [17], we focus in this work on the effect of nonlinearities in cyclostationary detection and assume perfect knowledge of the cyclic frequency. The lag ν at which the non-conjugate CAC is to be computed is modulation-dependent, and is set to $\nu = 0$ in this work as it maximizes the power of the cyclic feature at $\alpha = 2f_{IF}$.

Energy detection (ED) on the other hand can be seen as a special case of the CAC, and can be performed by computing the conjugate CAC at cyclic frequency $\alpha = 0$ and lag $\nu = 0$. In addition, we do not consider the noise uncertainty problem of EDs [6], and show the degradation of ED due to receiver nonlinearities only. The detector therefore computes the test statistic given by

$$R_{y^*}^0(0) = \frac{1}{N} \sum_{n=0}^{N-1} y[n]y[n]^*. \qquad (7)$$

Therefore, depending on the kind of detector, the sensing radio computes $R_y^\alpha(0)$ or $R_{y^*}^0(0)$, and performs the following hypothesis test

$$\text{Cyclic Detector} \begin{cases} |R_y^\alpha(0)| < \gamma_{CD} \rightarrow \text{SOI is absent} \\ |R_y^\alpha(0)| > \gamma_{CD} \rightarrow \text{SOI is present,} \end{cases}$$

$$\text{Energy Detector} \begin{cases} |R_{y^*}^0(0)| < \gamma_{ED} \rightarrow \text{SOI is absent} \\ |R_{y^*}^0(0)| > \gamma_{ED} \rightarrow \text{SOI is present.} \end{cases}$$

where γ is the decision threshold that is usually set to maintain a Constant Probability of False Alarm (CFAR) $P_{cfar} = \mathbb{P}(|R_y^\alpha(0)| > \gamma_{CD}|\mathcal{H}_0)$ under CD, or $P_{cfar} = \mathbb{P}(|R_{y^*}^0(0)| > \gamma_{ED}|\mathcal{H}_0)$ under ED.

B. Detection Performance Degradation under RF front-end nonlinearity

We analyze in this section the detection performance degradation of both detectors in the presence of third-order nonlinearities and strong blockers via simulation. In particular,
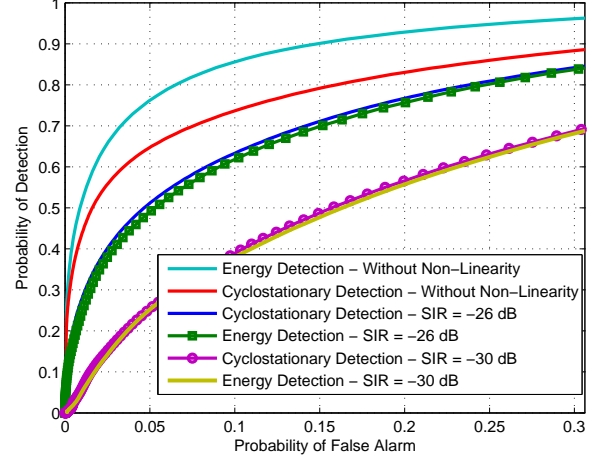

Fig. 2. Detection performance degradation of both cyclostationary-based and energy-based detectors in the presence of third-order nonlinearities with varying blocker strengths.

we focus on low SIR regimes, where the blockers power is much larger than the SOI power (when present). Fig. 2 shows the performance loss of both cyclostationary and energy-based detectors at a SNR of 0 dB using 5000 samples to compute (6) and (7). The IIP3 of the front-end of the Rx is -10dBm and the mean power of the wideband received signal is varied between three cases where there is no blocker, SIR = -26 dB and SIR = -30 dB. Fig. 2 shows simulated ROC for these three cases. Under no noise uncertainty [6], ED outperforms CD when the LNA operates in its linear region. However, the performances of both ED and CD degrade heavily when the Rx front-end operates in its nonlinear region. Although ED outperforms CD in case of a linear front-end, this advantage vanishes as the RF font-end operates in its non-linear regime. In the next section, we formulate an adaptive interference cancellation algorithm that improves the detection performance of both sensing algorithms under RF nonlinearities.

IV. ADAPTIVE INTERFERENCE CANCELLATION (AIC) ALGORITHM

In this section, we formulate an adaptive interference cancellation based approach for improving the sensing of weak signals in the presence of nonlinearities. The basic compensation structure, motivated by (1), is presented in Fig. 3. For every sensing operation, the band-split filtering stage first separates the subband of interest from rest of the band. These effective filtering functions are denoted by H_D and H_R with their corresponding impulse responses $h_D[n]$ and $h_R[n]$, respectively. Here, "D" refers to "desired" and "R" to "reference" signal branches.

Filtering the wideband signal $y_W[n]$ using the band-splitting filters yields

$$y[n] = h_D[n] * y_W[n] \approx x_D[n] + v_D[n]$$
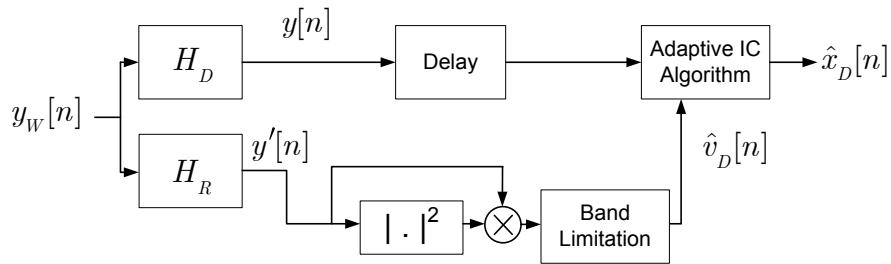$$y'[n] = h_R[n] * y_W[n] \approx x_R[n], \qquad (8)$$

Fig. 3. Proposed compensation structure for third-order nonlinearity in the front-end. The upper branch captures the desired signal subband and the lower branch generates an interference reference. These two signals are then processed by an adaptive interference canceller to suppress the nonlinear distortion effects from the signal of interest

where $*$ represents the convolution operation. Here $y_W[n]$ is the wideband signal in (1). Moreover, in (8), $y[n]$ is the signal residing at the subband of interest. In the two blocker case and modeling in (3) the blocker-free signal is $x_D[n] = \beta_1 z_0[n]e^{j2\pi f_{IF}nT_s} + w_z[n]$. The signal $y'[n]$ contains the components at the rest of the band, which we assume here to be dominated by the strong blockers. The spurious frequencies stemming from nonlinear component in the subband of interest are denoted by $v_D[n]$. Again, in the two-blockers case in (3) $v_D[n] = \frac{3\beta_3}{2}z_i^2[n]z_j^*[n]e^{j2\pi f_{IF}nT_s}$. The idea in this compensation structure is to regenerate $v_D[n]$, i.e. the portion of the IMD terms which are generated by the dominant blockers, from the signal components available in the reference branch. Considering the baseband model of nonlinearity in (1) it is possible to conclude that all the IM terms which are generated by the blockers can be re-generated by transforming $y'[n]$ with a baseband model of front-end nonlinearity, i.e. $y'[n]|y'[n]|^2$. Naturally, this nonlinear model generates the interfering as well as non-interfering inter/cross-modulation terms, therefore a band-limitation filter is required to isolate the interfering inter/cross-modulation term, i.e. $\hat{v}_D[n]$ (Fig.3). After generation of $\hat{v}_D[n]$, an adaptive filtering stage is applied to "scale" the reproduced IMD components properly before being subtracted from the desired signal. This can be written as

$$\hat{x}_D[n] = y[n] - \frac{3}{2}q[n]\hat{v}_D[n]. \tag{9}$$

The adaptive filter coefficient, $q[n]$, can be adjusted, e.g., to minimize the power of the compensator output using the well-known least-mean-square (LMS) algorithm [18] as follows

$$q[n+1] = q[n] + \mu\hat{v}_D^*[n]\hat{x}_D[n] \tag{10}$$

where the output of the interference canceller, serving also as the error signal in learning, is $\hat{x}_D[n]$. Also, μ is the step-size for the coefficients update of the LMS algorithm. In practical implementation, the effective processing of different nonlinearity orders can be carried out individually by having parallel reference signal branches (reference nonlinearity and adaptive filter stage) for each order of interest. For instance, possible fifth-order nonlinearity in the LNA can be accommodated by adding a branch of simple fifth-order stage, i.e. $y'[n]|y'[n]|^4$, followed by a band limitation and adaptive filter stage in the reference branch. Thus, in general, it should be noted that

no detailed *a priori* knowledge of the nonlinearity of the front-end is basically needed. The reference nonlinearity section simply regenerates the interfering frequency components which are then further modified by the online adaptive filter stage, controlling the actual interference cancellation process. Furthermore, by adjusting the band-split filtering stage that separates the current sensing subband from the rest of the spectrum, this method is applicable regardless of the position of the sensing subband.

V. NUMERICAL RESULTS

In this section, we show the performance of the interference cancellation algorithm first by analyzing the convergence of the adaptive filter for various blocker levels. We then show the performance gains that can be achieved using the proposed AIC for both energy and cyclostationary detectors for varying sensing time and blocker strength. All signals are 6 MHz wide, and follow the 8-VSB modulation scheme which exhibits a cyclic feature at $\alpha = 2f_{IF}$.

A. Interference Cancellation Performance

In order to analyze the performance of the AIC, we first analyze the convergence of the adaptive algorithm. Given that the compensation is performed before the detection, we do not consider any specific detection method at this point yet. As per the nature of adaptive filters, the number of samples used for the AIC determines the convergence level of the adaptive algorithm. We show in Fig. 4 the evolution of the AIC coefficient $q[n]$ over time for a range of SIR levels ranging from -10 dB to -36 dB with a step size $\mu = 5 \times 10^{-5}$. In our simulations, we consider $\beta_1 = 1$, an IIP3 of -10 dBm, resulting in $\beta_3 = -133.33$. As the reference signal to the adaptive filter is proportional to the blocker strength, the convergence rate of the AIC is therefore inversely proportional to the SIR. As a result, one would expect that the improvement in the detection performance improves with lower SIR. This will be validated in the rest of the numerical results. In addition, the convergence rate is faster with lower SIR. This in turn forms the trade off between AIC run-time and actual sensing time. Although estimating the β_3 coefficient is not performed as frequently as the sensing stage, increasing the number of iterations of the AIC in turn reduces the throughput of the CR network. However, given that main objective of the sensing radio is to avoid interference caused to the primary users, it is therefore of
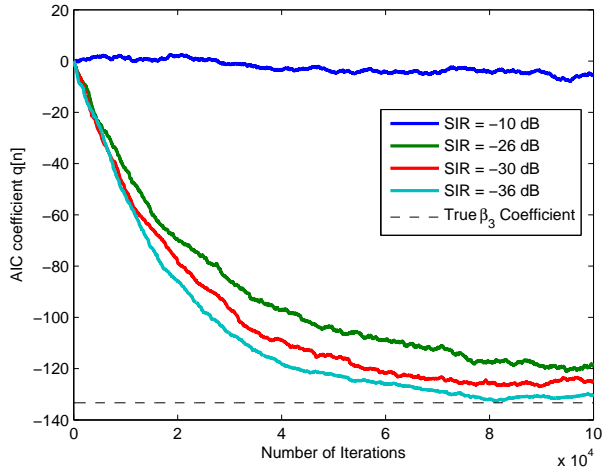
Fig. 4. The convergence behavior of the AIC algorithm coefficient, $q[n]$, for various levels of SIR under a SNR of 0 dB.
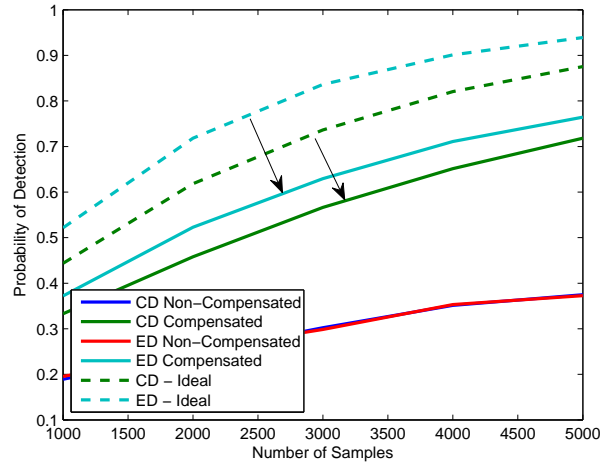

Fig. 5. Detection performance degradation of both cyclostationary-based and energy-based detectors with and without the AIC compensation as a function of the number of samples under an SIR of -30 dB and a SNR of 0 dB.

the interest of the SUs to compensate for the bad performance by running the AIC until convergence. To study the detection performance as a function of the remaining of the parameters, we select the number of iterations for the AIC to guarantee the convergence of the adaptive algorithm. In practice, e.g. normalized LMS learning or gear-shift type methods can offer better convergence in the coefficient adaptation.

B. Effect of Increasing Sensing Time

Next, we fix both the SNR to 0 dB, and the SIR to -30 dB, and vary the sensing time required to compute the test statistics. In fact, increasing the sensing time is equivalent to improving the SNR and SIR for both ED and CD as the variance of both the intermodulation term and the noise decrease with increasing N. Fig. 5 shows the detection probability for a fixed CFAR of 0.1 for varying number of samples N from 1000 to 5000 samples. At the SIR level of -30 dB, both non-compensated ED and CD perform similarly, and the detection probability increases with increasing N. After estimating β_3 using 10^5 samples and compensating for the effect of nonlinearities, energy detectors regain their advantage over cyclostationary detectors as the detection performance of ED becomes better than that of CD. In addition, we note that the performance gains due to the AIC increase with increasing sensing time. Further, we compare in Fig. 5 the detection performance of the compensated detectors with the performance of ideal detectors in the absence of nonlinearity. We make two observations. First, the performance of the compensated detectors is still worse than that of the ideal ones. In fact, as was shown in Section V-A, the convergence rate of the AIC is faster in low SIR regimes. Therefore, it is expected that the gap between compensated and ideal curves increases with increasing SIR levels. Second, as we have shown in Fig. 2 that ED suffers from a greater performance loss under nonlinearities, this behavior can also be seen in the performance degradation between compensated and ideal detection performance.

C. Varying Blocker Power

In this section, we analyze the performance gains of both energy and cyclostationary detectors in the presence of strong blockers for different SIR levels. The sensing time is fixed to $N = 5000$ samples, and the SNR is set to 0 dB. The SIR level is varied between -10 dB and -36 dB. Fig. 6 shows the ROC curve for cyclostationary detectors with and without the compensation. At high SIRs, the reference signal of the adaptive filter is weak as the intermodulation term has low power. As a result, the AIC fails to compensate for the non-linear effect of the LNA, and therefore the performance of both compensated and non-compensated CD coincide. However, with increasing blocker power, the AIC converges as the strength of the reference signal is relatively high. The performance gains due to the AIC increase with increasing blocker power, which is equivalent to decreasing SIR levels. On the other hand, Fig. 7 shows a similar behavior of ED in terms of the compensation levels as a function of the SIR. However, the performance of compensated CDs do not degrade as much as compensated ED from an SIR level of -10 dB to -26 dB. As a result, one can conclude that compensated cyclostationary detectors are more robust to weak blockers than compensated energy detectors.

VI. CONCLUSIONS

When the receiver LNA is operating in its non-linear regime, we showed in this paper that wideband spectrum sensing can suffer severe degradation in its detection performance in the presence of strong blockers. We have analyzed the effect of these nonlinearities on both cyclostationary detectors and energy detectors. We have proposed an interference cancellation based compensation method to subtract the effect of the blockers at any subband of interest by means of an adaptive algorithm whose performance has been evaluated numerically. The performance gains of both detectors with and without the compensation have been analyzed for varying blocker levels
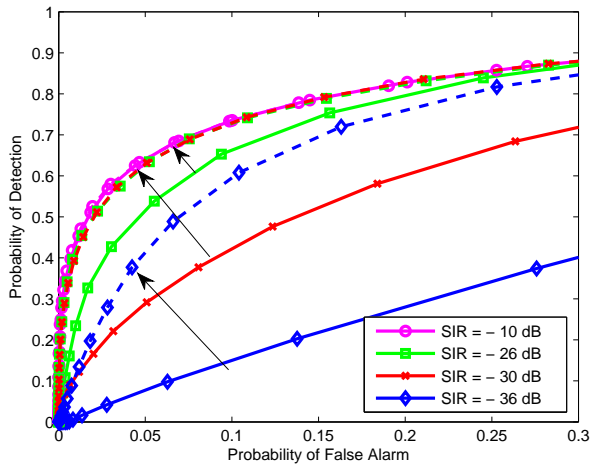
Fig. 6. ROC curves for compensated and non-compensated cyclostationary-based detectors in the presence of third-order nonlinearities with varying blocker strengths. Solid lines and dashed lines correspond to non-compensated and compensated ROC curves, respectively.
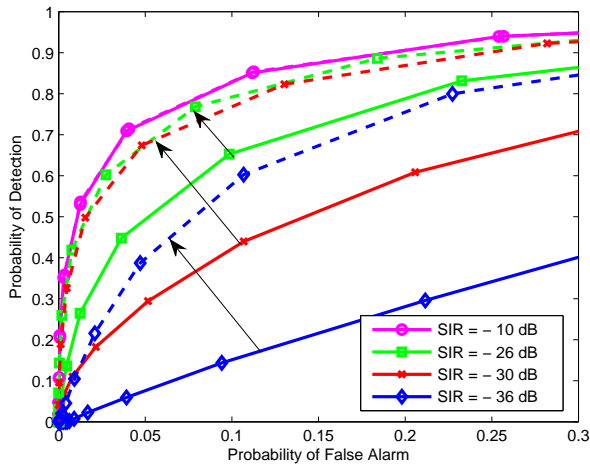

Fig. 7. ROC curves for compensated and non-compensated energy-based detectors in the presence of third-order nonlinearities with varying blocker strengths. Solid lines and dashed lines correspond to non-compensated and compensated ROC curves, respectively.

and sensing time. Without compensation, we have shown that energy detectors lose their advantage over cyclostationary detectors even in the absence of noise uncertainty. Further, we have shown that compensated cyclostationary detectors are more robust to weak blockers than compensated energy detectors. Overall, the results indicate that the developed adaptive interference cancellation approach can reduce the effects of RF nonlinearities in spectrum sensing receiver in a considerable manner.

REFERENCES

[1] J. Mitola III and G. Q. Maguire Jr., "Cognitive radio: making software radios more personal," *IEEE Personal Commun. Mag.*, vol. 6, no. 4, pp. 13–18, Aug. 1999.

[2] T. Yucek and H. Arslan, "A survey of spectrum sensing algorithms for cognitive radio applications," *IEEE Commun. Surveys Tuts.*, vol. 11, no. 1, pp. 116–130, First Quarter 2009.

[3] W. A. Gardner, *Statistical spectral analysis: a non probabilistic theory*. Prentice Hall, 1988.

[4] A. V. Dandawate and G. B. Giannakis, "Statistical tests for presence of cyclostationarity," *IEEE Trans. Sign. Proc.*, vol. 42, no. 9, pp. 2355–2369, Sep. 1994.

[5] D. Cabric, S. Mishra, and R. Brodersen, "Implementation issues in spectrum sensing for cognitive radios," in *Proc. ACSSC*, Pacific Grove, CA, USA, Nov. 7–10, 2004.

[6] R. Tandra and A. Sahai, "SNR walls for signal detection," *IEEE J. Sel. Topics Signal Process.*, vol. 2, no. 1, pp. 4–17, Feb. 2008.

[7] V. Syrjala, M. Valkama, N. Tchamov, and J. Rinne, "Phase noise modelling and mitigation techniques in OFDM communications systems," in *Proc. of Wireless Telecom. Symposium*, 2009, pp. 1 –7.

[8] M. Valkama, M. Renfors, and V. Koivunen, "Advanced methods for I/Q imbalance compensation in communication receivers," *IEEE Trans. Sign. Proc.*, vol. 49, no. 10, pp. 2335–2344, Oct. 2001.

[9] A. Zarashi-Ghasabeh, A. Tarighat, and B. Daneshrad, "Cyclo-stationary sensing of OFDM waveforms in the presence of receiver RF impairments," in *IEEE Proc. WCNC'10*, Apr.1–6 2010.

[10] J. Verlant-Chenet, J. Renard, J. Dricot, P. D. Doncker, and F. Horlin, "Sensitivity of spectrum sensing techniques to RF impairments," in *Proc. IEEE Veh. Techn. Conf. (VTC)*, May 2010, pp. 1–5.

[11] A. Shahed hagh ghadam, *Contributions to Analysis and DSP-based Mitigation of Nonlinear Distortion in Radio Transceivers*. Ph.D. dissertation, Tampere University of Technology, 2011.

[12] B. Razavi, "Cognitive radio design challenges and techniques," *IEEE J. Solid-State Circuits*, vol. 45, no. 8, pp. 1542–1553, Aug. 2010.

[13] D. Mahrof, E. A. M. Klumperink, J. C. Haartsen, and B. Nauta, "On the effect of spectral location of interferers on linearity requirements for wideband cognitive radio receivers," in *Proc. DySPAN*, Apr.1–9 2010.

[14] M. Valkama, A. Shahed hagh ghadam, L. Anttila, and M. Renfors, "Advanced digital signal processing techniques for compensation of nonlinear distortion in wideband multicarrier radio receivers," *IEEE Trans. Microw. Theory Tech.*, vol. 54, no. 6, pp. 2356–2366, Jun. 2006.

[15] Q. Zou, M. Mikhemar, and A. H. Sayed, "Digital compensation of cross-modulation distortion in software-defined radios," *IEEE Journal of Selected Topics in Signal Processing*, vol. 3, no. 32, pp. 348–361, Jun. 2009.

[16] Y. Zeng and Y. C. Liang, "Robustness of the cyclostationary detection to cyclic frequency mismatch," in *Proc. IEEE PIMRC*, Istanbul, Turkey, 2010.

[17] E. Rebeiz, P. Urriza, and D. Cabric, "Experimental analysis of cyclostationary detectors under cyclic frequency offsets," in *Proc. IEEE Asilomar Conference on Signals, Systems and Computers*, Pacific Grove, 2012.

[18] S. Haykin, *Adaptive Filter Theory*. 4th ed. Upper Saddle River, NJ: Prentice Hall, 2002.